Groundwater

MODFLOW-Based Coupled Surface Water Routing and Groundwater-Flow Simulation

by J.D. Hughes[1], C.D. Langevin[2], and J.T. White[3]

Abstract

In this paper, we present a flexible approach for simulating one- and two-dimensional routing of surface water using a numerical surface water routing (SWR) code implicitly coupled to the groundwater-flow process in MODFLOW. Surface water routing in SWR can be simulated using a diffusive-wave approximation of the Saint-Venant equations and/or a simplified level-pool approach. SWR can account for surface water flow controlled by backwater conditions caused by small water-surface gradients or surface water control structures. A number of typical surface water control structures, such as culverts, weirs, and gates, can be represented, and it is possible to implement operational rules to manage surface water stages and streamflow. The nonlinear system of surface water flow equations formulated in SWR is solved by using Newton methods and direct or iterative solvers. SWR was tested by simulating the (1) Lal axisymmetric overland flow, (2) V-catchment, and (3) modified Pinder-Sauer problems. Simulated results for these problems compare well with other published results and indicate that SWR provides accurate results for surface water-only and coupled surface water/groundwater problems. Results for an application of SWR and MODFLOW to the Snapper Creek area of Miami-Dade County, Florida, USA are also presented and demonstrate the value of coupled surface water and groundwater simulation in managed, low-relief coastal settings.

Introduction

Groundwater flow in unconfined, water table aquifers can be strongly affected by interaction with surface water (e.g., Lee et al. 2010). In areas where surface water flow is channelized and flow is predominantly caused by channel bed slope, surface water flow and aquifer interactions can be simulated with MODFLOW (Harbaugh 2005) using the streamflow-routing (SFR2) package (Niswonger and Prudic 2005). The SFR2 package solves for one-dimensional unidirectional channel flow for conditions where stream discharge is a function of the channel bed slope. Surface water flow may be bidirectional in areas where water-surface and channel bed slopes are less than or equal to 1.0×10^{-4} m/m (Hughes et al. 2012), managed by using pumps and control structures, and/or tidally influenced. In these settings, the SFR2 package will not accurately represent surface water flow conditions or aquifer exchanges.

To represent conditions where surface water flow may be bidirectional, two-dimensional, and/or highly managed, the surface water routing (SWR) numerical surface water code was developed and implicitly coupled to MODFLOW. Similar to the SFR2 package, SWR routes surface water based on a solution of the continuity equation for surface water flow. However, unlike the SFR2 package, SWR can also account for backwater effects, bidirectional surface water flow, two-dimensional flow, and management of surface water using control structures.

SWR was recently coupled to MODFLOW-NWT (Niswonger et al. 2011), a version of MODFLOW that is intended for solving nonlinear unconfined groundwater-flow problems. The underlying formulations of MODFLOW-NWT are the same as previous versions of MODFLOW (e.g., Harbaugh 2005) except for the option to apply upstream weighting to hydraulic conductance and add Newton correction terms to the conductance matrix and the right-hand side (RHS) of the groundwater-flow equation. In this paper, MODFLOW refers to MODFLOW-NWT.

The objective of this paper is to present a concise description of the mathematical formulation used to represent surface water flow and surface water/groundwater interactions. The methodology is presented in the context of the combined SWR and MODFLOW computer program. SWR has been tested with a number of surface

[1]Corresponding author: Florida Water Science Center, U.S. Geological Survey, 4446 Pet Lane Suite 108, Lutz, FL 33559; 813-498-5029; fax: 813-498-5002; jdhughes@usgs.gov

[2]U.S. Geological Survey, 411 National Center, Reston, VA 20192

[3]Texas Water Science Center, U.S. Geological Survey, 1505 Ferguson Lane, Austin, TX 78754

Received December 2013, accepted March 2014.

Published 2014. This article is a U.S. Government work and is in the public domain in the USA.

doi: 10.1111/gwat.12216

water flow problems (Hughes et al. 2012). In this paper, we present results for three additional numerically challenging tests—the Lal axisymmetric overland flow problem (Lal 1998), the tilted V-Catchment problem (Di Giammarco et al. 1996; Panday and Huyakorn 2004), and the modified Pinder-Sauer problem (Lal 2001) to demonstrate the level of accuracy that can be obtained with SWR and combined SWR-MODFLOW approaches. We also present results for a combined SWR-MODFLOW model of the Snapper Creek area of Miami-Dade County, Florida, to demonstrate application of the approach to a field setting.

Model Description

This section describes the mathematical model of surface water flow and surface water/groundwater interaction, finite volume form of the surface water flow equation, coupling of the surface water and groundwater codes, and program structure.

Mathematical Model of Surface Water Flow

The full Saint-Venant equations represent a coupled system of equations that includes the continuity and conservation of momentum equations. The diffusive-wave approximation of the Saint-Venant equations represents a simplification of the full equations and is applied in SWR. The diffusive-wave approximation is formulated using a simplification of the conservation of momentum equation:

$$\overbrace{\frac{\partial Q}{\partial t}}^{1} + \overbrace{\frac{\partial}{\partial x}\left(\frac{\beta Q^2}{A}\right)}^{2} + \overbrace{gA\left(S_f + \frac{\partial h}{\partial x}\right)}^{3} + \overbrace{M_{SRC}}^{4} = 0, \quad (1)$$

where Q is streamflow [L^3/T], t represents time [T], x represents the spatial coordinates [L], β is a momentum correction factor [unitless], A is the cross-sectional area [L^2], g is the gravitational acceleration [L/T^2], S_f is the friction slope [L/L], h is the surface water stage [L], and M_{SRC} is the momentum change due to source and sink terms [L^3/T^2]. Examples of source and sink terms include lateral inflow (runoff), aquifer exchanges, and internal flow terms (such as instream and/or laterally connected surface water control structures). A direct relation of S_f to the water-surface gradient is defined if Equation 1 is simplified by ignoring terms 1, 2, and 4. Substitution of the third term in Equation 1 with Manning's equation into the continuity equation in terms of flow per unit length results in

$$\frac{\partial A}{\partial t} + \frac{\partial}{\partial x}\left(\frac{1}{n}\frac{A}{\left|\frac{\partial h}{\partial s}\right|^{1/2}}\left(\frac{A}{P}\right)^{2/3}\frac{\partial h}{\partial x}\right) + q_{SRC} = 0, \quad (2)$$

where n is the Gauckler-Manning-Strickler roughness coefficient [$T/L^{1/3}$], s is the relative spatial coordinate [L] in the direction of maximum local stage gradient, P is the wetted perimeter [L], and q_{SRC} is the volumetric flow rate of internal and external source and sink terms per unit length [L^3/TL]. For one-dimensional problems, $\frac{\partial h}{\partial s} = \frac{\partial h}{\partial x}$. Full derivation of the diffusive-wave approximation of the Saint-Venant equations can be found in the work of Feng and Molz (1997).

The surface water and groundwater domains are dynamically coupled through the q_{SRC} term in Equation 2, which can include an aquifer exchange term. Aquifer exchange, q_{AQ}, is calculated using

$$q_{AQ} = L\frac{H - h}{\partial z}, \quad (3)$$

where L is the leakance coefficient [L/TL], H is the groundwater head [L], and z is elevation of the top and bottom of bed sediments separating a surface water feature from the aquifer [L].

Numerical Approach of Surface Water Flow

SWR uses a finite-volume approach to discretize Equation 2 for arbitrary one-dimensional and rectilinear two-dimensional surface water features. The control volume for a surface water feature is called a reach. Volumetric fluid source and sink terms [L^3/T] represented in SWR include: (1) instream and lateral surface water control structure flow, Q_{STR}; (2) point and nonpoint source lateral inflow and outflow, Q_{LAT}; (3) rainfall, Q_{RAI}; (4) evapotranspiration, Q_{EVT}; (5) reach-aquifer exchanges, Q_{AQ}; and (6) exchanges with external boundaries (specified-stage reaches and/or stage-dependent boundaries), Q_{EX}. Discretization of Equation 2 in volumetric terms with internal and external fluid source and sink terms results in

$$\frac{\Delta V}{\Delta t} + \sum_{i=1}^{nuc}\left(\frac{c}{\overline{n}_i}\frac{\overline{A}_i}{\left|\frac{\Delta h_i}{\Delta s_i}\right|^{1/2}}\left(\frac{\overline{A}_i}{\overline{P}_i}\right)^{2/3}\frac{\Delta h_i}{\Delta x_i}\right) + \sum_{j=1}^{nsc} Q_{STR_j} + Q_{LAT} + Q_{RAI} + Q_{EVT} + Q_{AQ} + Q_{EX} = R = 0, \quad (4)$$

where V is the volume of water in a reach [L^3], nuc is the number of unmanaged reaches connected to the current reach, c is a unit conversion factor for the Gauckler-Manning-Strickler roughness coefficient [unitless], $\overline{n}$ is the distance-weighted Gauckler-Manning-Strickler roughness coefficient [$T/L^{1/3}$], $\overline{A}$ is the distance-weighted cross-sectional area [L^2], $\overline{P}$ is the distance-weighted wetted perimeter [L], nsc is the number of surface water control structures connected to the current reach, and R is the residual of the continuity equation [L^3/T].

In SWR, surface water flow between connected reaches is calculated using the diffusive-wave approximation of the Saint-Venant equations except where connected reaches are separated by one or more surface water control structures. Surface water control equations that can be simulated include fixed culverts and operable

17456584, 2015, 3, Downloaded from https://ngwa.onlinelibrary.wiley.com/doi/10.1111/gwat.12216 by U.S. Geological Survey Library, Wiley Online Library on [03/04/2024]. See the Terms and Conditions (https://onlinelibrary.wiley.com/terms-and-conditions) on Wiley Online Library for rules of use; OA articles are governed by the applicable Creative Commons License

pumps, weirs, and gates. Specification of surface water control structures at every connection for a given reach reduces SWR to a simpler level-pool approximation of surface water flow (Zoppou 1999; Hughes et al. 2012). Two-dimensional flow can be represented using reach geometries and connectivity defined using land-surface elevations and/or bathymetry discretized by a rectilinear grid. Each two-dimensional reach is connected to no more than four surrounding reaches and may be separated from surrounding reaches by surface water control structures.

The flexible formulation of SWR allows many different types of surface water features to be simulated and coupled with an underlying aquifer system. For example, SWR can be used to represent flowing rivers and streams, irrigation and other types of managed canals, and multi- or single-cell lakes and wetlands. Water can also be routed between the different surface water features to more accurately represent realistic surface water flow patterns. Hughes et al. (2012) describe the use of SWR as an alternative to other MODFLOW packages.

A standard conductance approach is used to calculate reach-aquifer exchanges. In its simplest form Q_{AQ} is calculated using

$$Q_{\mathrm{AQ}} = C\,(H - h) = LP\Delta x\,(H - h)\,, \qquad (5)$$

where C is reach-bed conductance [L^2/T]. In SWR, it is possible to calculate Q_{AQ} using (1) a specified value of C; (2) C calculated using L and P; (3) C calculated using a reach-transmissivity approach that depends on hydraulic conductivity (K) and P; or (4) a weighted combination of the L and reach-transmissivity approaches. Readers are referred to the work of Chin (1991) or Nemeth and Solo-Gabriele (2003) for additional details on the reach-transmissivity approach.

Newton methods are used to solve the discretized nonlinear system of equations at each SWR time step. In this method, the coupled nonlinear system of equations is solved by first applying a Newton linearization, then using either direct or iterative Krylov methods to solve the resulting Jacobian system for each Newton iteration. The Jacobian of the nonlinear Equation 4 is approximated by a first-order finite-difference approximation. Newton iterations are continued until user-specified stage (Δh) and flow (R) criteria are satisfied. The SWR system of equations is solved for one or more SWR time steps in a MODFLOW time step. Additional details on the numerical methods implemented in the SWR and available options (e.g., adaptive time stepping) can be found in the work of Hughes et al. (2012).

Coupling SWR and MODFLOW

SWR is incorporated into MODFLOW similar to other head-dependent boundary condition packages, with head-dependent flow terms in Equation 5 added to the diagonal of the conductance matrix (HCOF) and RHS vector of the groundwater-flow equation. Optionally, groundwater heads are perturbed in SWR to calculate first-order finite-difference reach-aquifer exchange derivatives that are also added to HCOF and RHS (Niswonger et al. 2011). Groundwater heads from the last nonlinear MODFLOW outer iteration or previous MODFLOW time step are used to calculate Q_{AQ} during each SWR time step. The SWR equations are solved for each MODFLOW outer iteration, and these outer iterations continue until standard head and flow convergence criteria are met and optional reach-cell exchange convergence criteria are met.

Although not explored in this paper, the MODFLOW unsaturated zone flow (UZF) package (Niswonger et al. 2006) and SWR can be used concurrently in a model to simulate infiltration- and/or saturation-excess hydrologic processes, collection of surface water runoff from the landscape in surface water conveyances, and SWR on the landscape. Unlike SFR2, however, the current SWR implementation does not support unsaturated zone flow beneath surface water features. Coupling of SWR and the UZF package is described in more detail in the work of Hughes et al. (2012).

Inclusion of SWR in MODFLOW also permits additional coupling with other MODFLOW packages and processes. For example, SWR has recently been coupled to subsidence packages available in MODFLOW (Höffmann et al. 2003; Leake and Galloway 2007) so that subsidence-induced changes in river/canal bottom elevations and structure inverts can be dynamically simulated; the ability to simulate groundwater-pumpage-induced changes in surface water conveyances can be important in many agricultural areas (e.g., the Central Valley of California; Faunt 2009). SWR has also recently been coupled to the farm process for MODFLOW to provide an alternative to the SFR2 package to simulate deliveries to and return flows from low-gradient, managed agricultural areas (Schmid et al. 2006).

Code Evaluation

SWR has been tested with a number of steady and unsteady one- and two-dimensional surface water flow problems. The numerical approach has been applied by Hughes et al. (2011) to a number of two-dimensional low-gradient hypothetical and field problems using a previous version of SWR. SWR results have also been compared with results from other codes for a number of hypothetical one- and two-dimensional surface water flow problems (Hughes et al. 2012). In this section, SWR is tested with two additional numerically challenging surface water problems: the axisymmetric overland flow problem and the tilted V-Catchment problem. The coupling of SWR and MODFLOW is also tested using the modified Pinder-Sauer problem to evaluate the ability of SWR to simulated transient surface water flow and surface water/groundwater exchanges. Differences between SWR and other results are quantified using

$$\mathrm{ME} = \frac{1}{n}\sum_{i=1}^{\mathrm{nobs}} (v_{\mathrm{SWR}} - v_c)_i\,, \qquad (6)$$

17456584, 2015, 3, Downloaded from https://ngwa.onlinelibrary.wiley.com/doi/10.1111/gwat.12216 by U.S. Geological Survey Library, Wiley Online Library on [03/04/2024]. See the Terms and Conditions (https://onlinelibrary.wiley.com/terms-and-conditions) on Wiley Online Library for rules of use; OA articles are governed by the applicable Creative Commons License

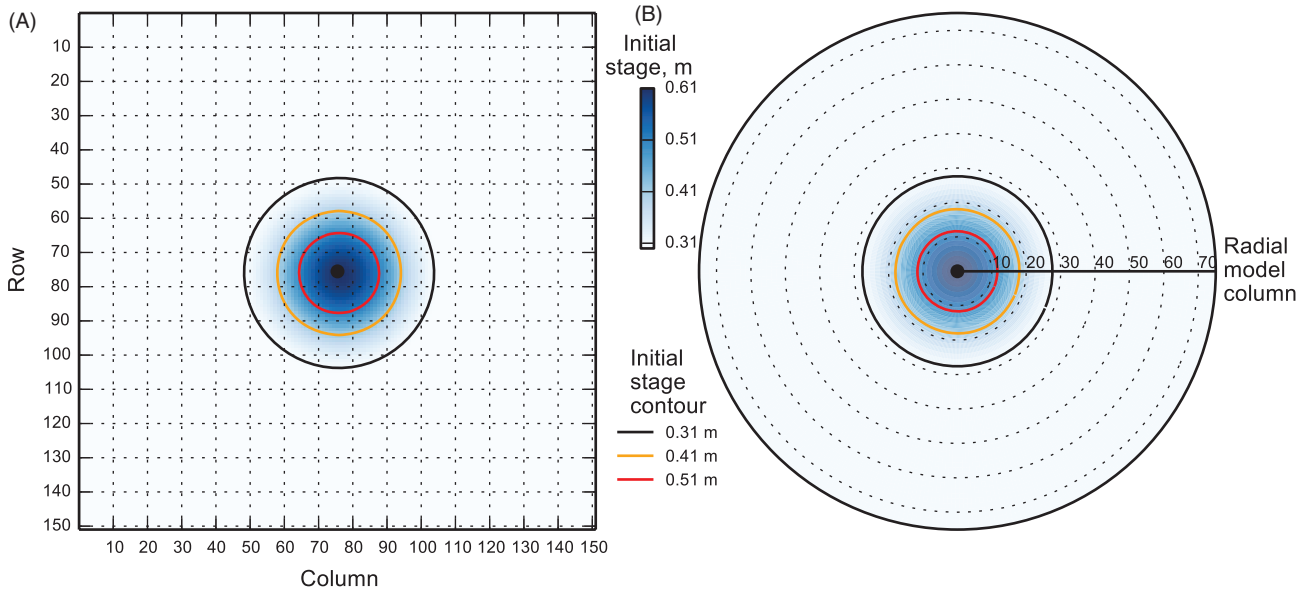

Figure 1. (A) 151 row × 151 column rectilinear model grid used to evaluate the axisymmetric overland flow problem. (B) 1 row × 75 column radial model grid used to evaluate the accuracy of the axisymmetric overland flow problem solved using a rectilinear grid. Every 10th row and column is shown in (A) and every 10th column is shown in (B). Initial surface water stages are also shown.

where ME is the mean error, nobs is the number of observations, v_{SWR} is SWR result i, and v_c is result i that SWR results are being compared to. Differences between SWR and other results are also quantified using

$$\mathrm{RMSE} = \left[\frac{1}{n}\sum_{i=1}^{\mathrm{nobs}}(v_{\mathrm{SWR}} - v_c)_i^2\right]^{0.5}, \qquad (7)$$

where RMSE is the root mean square error (or standard deviation). Results compared with SWR results were linearly interpolated to SWR simulation times in cases where output times did not coincide.

Axisymmetric Overland Flow Problem

An axisymmetric overland flow problem developed by Lal (1998) was used to test SWR. This problem simulates axisymmetric overland flow and the transient decay of a symmetric surface water mound.

The model domain represents an overland flow plane that is 161,000 × 161,000 m. Groundwater is not considered in this test problem (by inactivating all MODFLOW cells). The overland flow plane is horizontal and specified to have an elevation of 0.0 m. The initial water-surface stage is

$$h = \left[0.4575 + 0.1525\cos\left(\frac{\pi r}{r_{\max}}\right)\right] \text{ for } r \le r_{\max}, \qquad (8)$$

where r is the distance from the domain center and $r_{\max}$ is 32,188 m (Figure 1). At distances greater than $r_{\max}$ the initial surface water stage is 0.305 m. Constant stage boundaries were specified on all sides at the edge of the model domain and were specified to be 0.305 m.

A constant Gauckler-Manning-Strickler roughness coefficient of 1.0 s/m$^{1/3}$ was specified. Rainfall, evaporation, and lateral inflows were specified to be zero.

The square 161,000 × 161,000 m model domain was discretized using a uniform grid with a total of 151 rows, 151 columns (Figure 1A). A constant grid spacing of 1072.90 m was used for each row and column. The total simulation length was 288 h and a constant time-step length of 1 h was used.

Simulated results showing the edge of the surface water mound (0.31 m contour) after 0, 50, 100, 150, 200, 255, and 288 h are shown in Figure 2A. Simulated water levels at $r = 0.0$ m (Obs. 1), $r = 11,801.9$ m (Obs. 2), and $r = 31,114.1$ m are shown in Figure 2B. SWR results are compared with results calculated using SWIFT2D (Schaffranek 2004). In general, SWR and SWIFT2D results are comparable at the three observation locations. The ME and RMSE for 432 paired results are 0.0034 and 0.0038 m, respectively. SWIFT2D uses surface water stage gradients between cells rather than the surface water stage gradients in the direction of maximum local stage slope ($\frac{\partial h}{\partial s}$) to calculate Q_M terms for each cell (see Equation 2) and as a result is less accurate than SWR for axisymmetric problems.

A radial model was also developed to evaluate the accuracy of the SWR solution of the axisymmetric problem on a rectilinear grid (Figure 1B). A total of 1 row and 76 columns, with a constant grid spacing of 1,072.90 m, were used to discretize the radial model domain. The radial model included a total of 76 SWR reaches with a constant reach length of 1072.90 m (in the radial direction from the center of the model domain located in the first column) and variable reach widths equal to the perimeter of the radial model domain at the

17456584, 2015, 3, Downloaded from https://ngwa.onlinelibrary.wiley.com/doi/10.1111/gwat.12216 by U.S. Geological Survey Library, Wiley Online Library on [03/04/2024]. See the Terms and Conditions (https://onlinelibrary.wiley.com/terms-and-conditions) on Wiley Online Library for rules of use; OA articles are governed by the applicable Creative Commons License

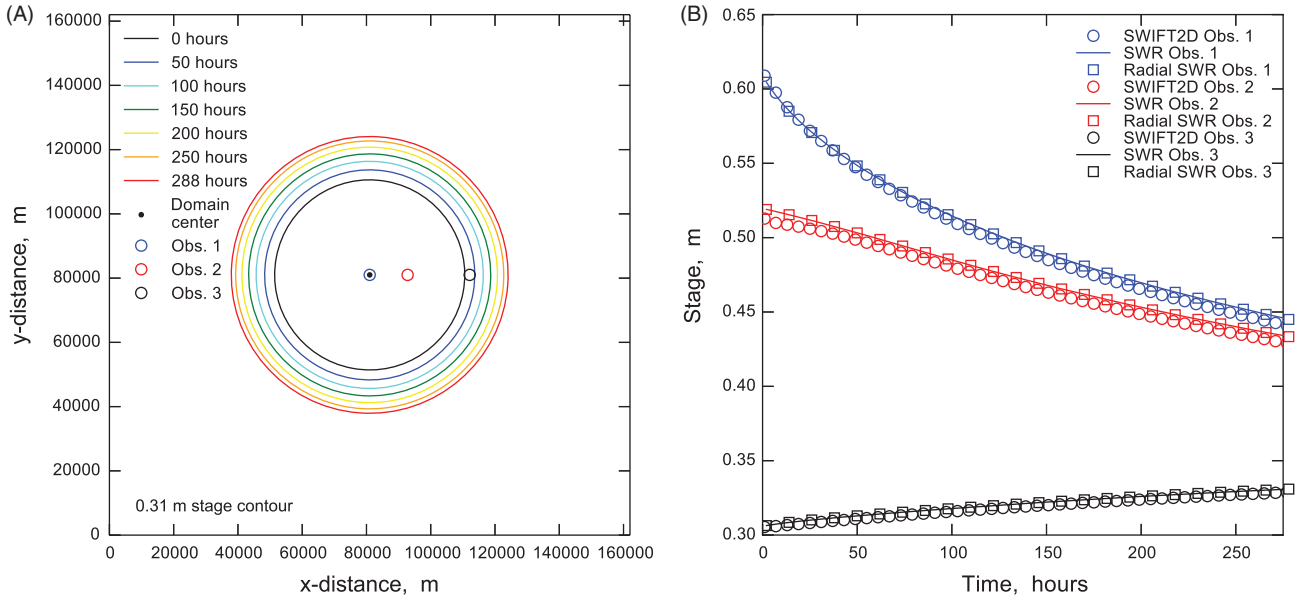

Figure 2. (A) Simulated decay of the surface water stage after 50, 100, 150, 200, 250, and 288 h. Initial surface water stage and the location of three observation locations are also shown in (A). (B) Comparison of SWR and SWIFT2D axisymmetric model results at observation locations 1, 2, and 3. SWR results from the rectilinear and radial models are also compared.

center of each reach (Figure 1B). Reach widths ranged from 842.65 to 505,592.21 m at the center of the first and last reach, respectively. Differences between MODFLOW model grid dimensions and radial SWR reach dimensions do not present a problem in the radial model because groundwater flow is not considered. All other parameters were the same as used in the 151 row × 151 column SWR model. Simulated results for the radial SWR model at the three observation locations are also shown on Figure 2B. Radial model results are nearly identical to the 151 row × 151 column SWR model (ME = 0.00009 m and RMSE = 0.00012 m) and demonstrate that SWR can accurately simulate axisymmetric problems using a rectilinear grid.

Tilted V-Catchment Problem

A two-dimensional overland flow problem on a tilted V-catchment as simulated by Di Giammarco et al. (1996) and Panday and Huyakorn (2004) was used to test SWR. This problem consists of overland flow generated in response to a rainfall event.

The tilted V-catchment includes two overland flow planes that are 1000 m long × 800 m wide separated by a 20-m-wide channel. Groundwater is not considered in this test problem (by inactivating all MODFLOW cells). Each overland flow plane slopes 0.05 in the x-direction (perpendicular to the channel) and 0.02 in the y-direction (parallel to the channel). The channel has a slope of 0.02 and is 1 m below adjacent overland flow plane cells. As a result of the symmetry of the problem only one half of the tilted V-catchment is simulated (Figure 3A) and discharge results are doubled to produce equivalent results.

Constant Gauckler-Manning-Strickler roughness coefficients of 0.015 and 0.15 $s/m^{1/3}$ were specified for the overland flow plane and the channel, respectively. Although these Gauckler-Manning-Strickler roughness coefficients are unrealistic they were used to facilitate comparison with previous solutions (Di Giammarco et al. 1996; Panday and Huyakorn 2004).

No-flow boundaries were specified at the edge of the model domain except at the downstream end of the channel where a critical-depth ($Q_{EX} = \left(gA^2R\right)^{\frac{1}{2}}$) boundary was specified. A critical-depth boundary condition defines the depth at the boundary to be the critical depth under free-fall conditions (downstream stage at the boundary is below the reach bottom). Critical-depth boundaries were also specified where the overland flow plane connects to the channel. Rainfall was applied at a rate of 3×10^{-6} m/s to the overland flow plane and the channel for 90 min with 0 m/s of rainfall applied for the remainder of the simulation. Evaporation and lateral inflows were specified to be zero. Initially the overland flood plane and channel were specified to be dry.

A total of 20 rows and 17 columns were used to discretize the model domain. A constant grid spacing of 50 m was used for each row. A constant grid spacing of 50 m was specified for columns 1–16. A 10-m grid spacing was specified for column 17 to represent 1/2 of a rectangular channel. The total simulation length was 180 min and a constant time-step length of 10 s was used. The area and wetted perimeter in Equation 4 were upstream weighted because of the relatively steep slope of the overland flow plane and to facilitate comparison with published results.

Simulated discharge results at the downstream end of the channel are shown in Figure 3B. SWR compares well to the results of Di Giammarco et al. (1996) and Panday and Huyakorn (2004) at nearly all times and demonstrates

17456584, 2015, 3, Downloaded from https://ngwa.onlinelibrary.wiley.com/doi/10.1111/gwat.12216 by U.S. Geological Survey Library, Wiley Online Library on [03/04/2024]. See the Terms and Conditions (https://onlinelibrary.wiley.com/terms-and-conditions) on Wiley Online Library for rules of use; OA articles are governed by the applicable Creative Commons License

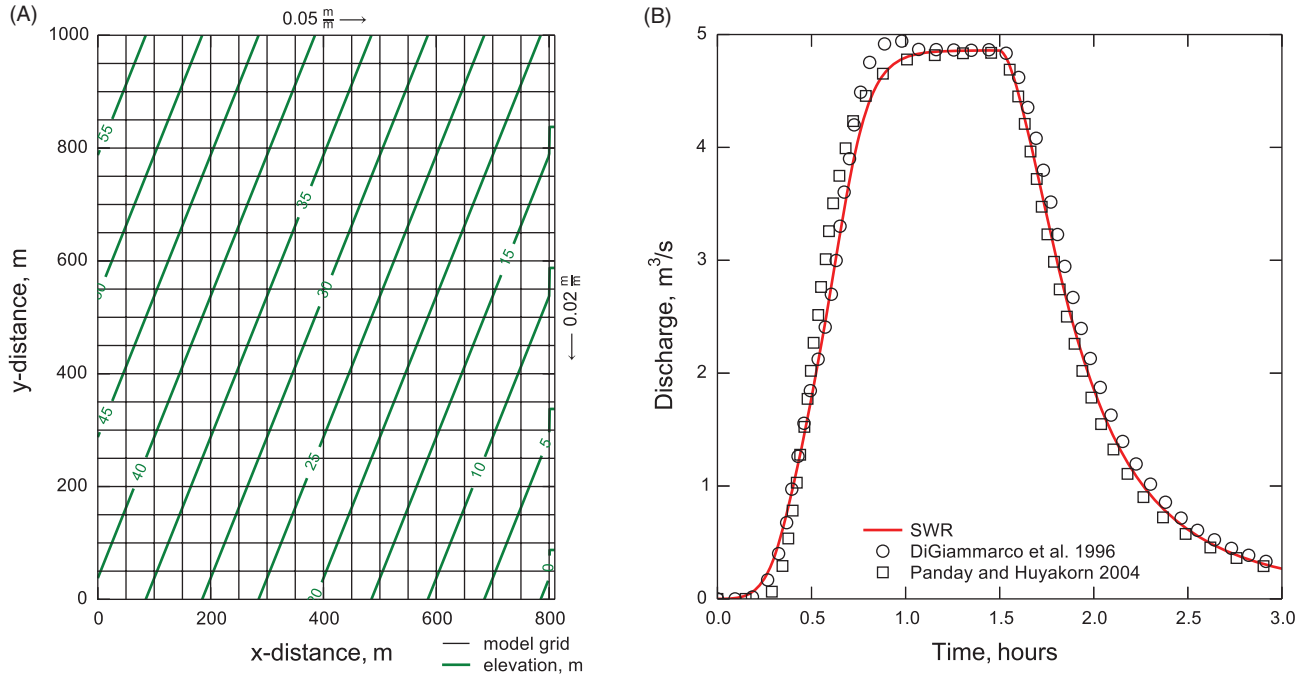

Figure 3. (A) Dimensions and overland flow plane elevations and gradient of the V-catchment problem. The V-catchment model grid is also shown in (A). (B) Comparison of SWR and the results of Di Giammarco et al. (1996) and Panday and Huyakorn (2004).

that SWR is able to simulate two-dimensional overland and one-dimensional channel flow in catchments with time-varying rainfall forcing. The ME and RMSE for 1080 paired SWR and Di Giammarco et al. (1996) results are −0.0871 and 0.1362 m^3/s, respectively. For 1080 paired SWR and Panday and Huyakorn (2004) results, the ME and RMSE are −0.0126 and 0.1712 m^3/s, respectively. The largest discrepancy between SWR and Di Giammarco et al. (1996) occurs at the top of the rising limb of the hydrograph; the largest discrepancy between Panday and Huyakorn (2004) and Di Giammarco et al. (1996) also occurs at the top of the rising limb of the hydrograph and suggests that this discrepancy may be a result of the numerical methods used to simulate surface water flow (Di Giammarco et al. [1996] use finite-element methods and both SWR and Panday and Huyakorn [2004] use finite-volume methods).

Modified Pinder-Sauer Problem

The modified Pinder-Sauer is a surface water/groundwater exchange problem that is based on the problem of Pinder and Sauer (1971), which has been used as a benchmark test for coupled surface water/groundwater models (e.g., Swain and Wexler 1996). Lal (2001) modified the problem of Pinder and Sauer (1971) to make it easier to set up and to include a sinusoidal inflow hydrograph boundary condition at the upstream end of the surface water system.

The model domain represents a flood plane that is 39,624 m long, 427 m across the valley, and underlain by an unconfined aquifer. The flood plane and underlying aquifer are surrounded by impermeable boundaries on all sides. The base of the aquifer is horizontal and specified to be at an elevation of 0.0 m. The flow direction in the model domain is along the long axis of the model from top to bottom.

The hydraulic conductivity of the aquifer is 3.048×10^{-3} m/s and the specific storage and specific yield are 0.25. Initially, the saturated thicknesses of the aquifer are 67.05 and 27.43 m at the upstream and downstream ends of the aquifer, respectively.

A single river channel is located at the center of the aquifer (column 8) parallel to the long axis of the model domain. The channel has a bed slope of 0.001, a width of 30.48 m, and a Gauckler-Manning-Strickler roughness coefficient of 0.03858 $s/m^{1/3}$. The uniform flow depth computed for a discharge rate of 509.7 m^3/s in the canal is 6.09 m. The hydraulic radius (A/P in Equation 2) is assumed to equal the actual canal depth. The leakage coefficient is 1.402×10^{-4}/s and seepage is assumed to occur only from the bottom.

The sinusoidal flood hydrograph introduced at the upstream boundary is

$$Q = 509.70 + 141.58 \sin\left(\frac{2\pi t}{T_p}\right), \qquad (9)$$

where T_p is the period of disturbance (s) and t is the simulation time (s). A T_p value of 5 h (18,000 s) was used. The downstream boundary is assumed to have uniform water-surface slope (zero-depth gradient) of 0.001.

A total of 65 rows, 15 columns, and 1 layer were used to discretize the model domain. A constant grid spacing of 609.61 m was used for each row. A grid spacing

17456584, 2015, 3, Downloaded from https://ngwa.onlinelibrary.wiley.com/doi/10.1111/gwat.12216 by U.S. Geological Survey Library, Wiley Online Library on [03/04/2024]. See the Terms and Conditions (https://onlinelibrary.wiley.com/terms-and-conditions) on Wiley Online Library for rules of use; OA articles are governed by the applicable Creative Commons License

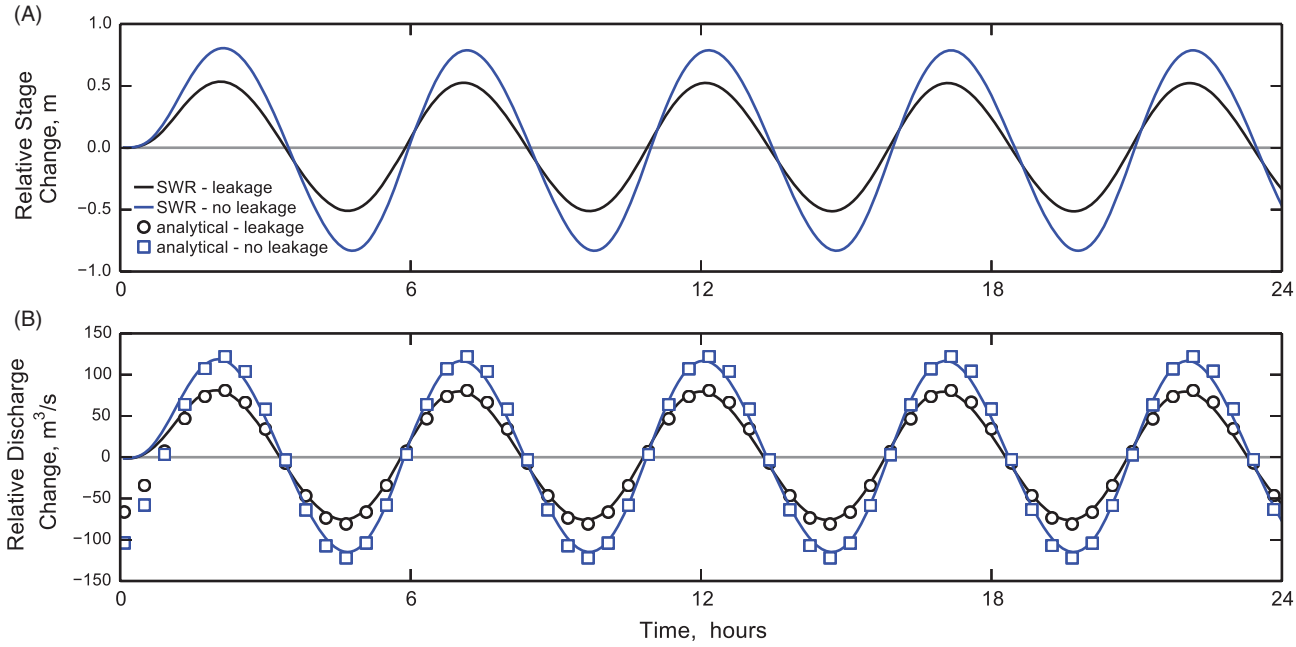

Figure 4. (A) Simulated relative stage change 15,240 m downstream of the top end of the model domain with and without aquifer exchange (leakage) for the modified Pinder-Sauer problem. (B) Comparison of relative discharge change 15,240 m downstream of the top end of the model domain and the analytical solution of Lal (2001) with and without aquifer exchange (leakage).

of 28.30 m was used for all columns except the center column (column 8); the grid spacing of column 8 was 30.48 m. The total simulation length was 24 h and a constant time-step length of 5 min was used for both SWR and MODFLOW.

Simulated relative stage and discharge results 15,240 m downstream of the top end of the model domain are shown in Figure 4. Relative stage and discharge results were calculated using the initial stage and discharge of 52.12 m and 509.70 m^3/s, respectively. For comparison, simulated relative stage and discharge for a simulation without aquifer exchange (leakage coefficient = 0.00/s) are also shown in Figure 4.

Lal (2001) developed an analytical solution for the discharge at a distance x from the upstream boundary as

$$Q_a = 509.70 + 141.58 \exp\left(\frac{\widehat{\lambda}_1 x}{\Lambda}\right) \sin\left(f_r t + \frac{\widehat{\lambda}_2 x}{\Lambda}\right), \quad (10)$$

where f_r is the characteristic frequency of the system, $\widehat{\lambda}_1$ is the amplitude decay constant, Λ is the characteristic length related to the wave number of the water-level disturbance, and $\widehat{\lambda}_2$ is a dimensionless wave number. The terms in Equation 10 are calculated using model parameters such as friction slope, reach sediment hydraulic conductivity, reach width; the parameters used to calculate terms in Equation 10 are defined in Lal (2001). For the case with aquifer exchange, the appropriate values for the variables in Equation 10 are $\widehat{\lambda}_1 = 0.1785$, $\Lambda = 4894.3$ m, $f_r = 3,49 \times 10^{-4}$/s, and $\widehat{\lambda}_2 = -0.3409$. Without aquifer exchange, $\widehat{\lambda}_1 = -4.779 \times 10^{-2}$, $\widehat{\lambda}_2 = -0.3608$, and all other variables are the same as the case with aquifer exchange.

Analytical results calculated using Equation 10 15,240 m downstream of the top end of the model domain are also shown in Figure 4; SWR results are comparable to the analytical solution. The numerical model requires a short warm-up period (less than 3 h) for surface water stage, surface water discharge, and groundwater levels to be consistent with the periodic upstream boundary (Equation 9); the analytical solution does not require a warm-up period. The ME and RMSE for relative discharge with aquifer exchange for 258 paired SWR and analytical results are −0.3223 and 4.6619 m^3/s, respectively. The ME and RMSE for relative discharge with no aquifer exchange for 258 paired SWR and analytical results are −0.3475 and 6.7250 m^3/s, respectively. Results for the first 2.5 h of the simulation (warm-up period) were excluded from the ME and RMSE calculations.

Snapper Creek Area of Miami-Dade County, Florida, USA

A combined SWR-MODFLOW model was developed for an area of Miami-Dade County that includes Snapper Creek and is shown in Figure 5. The purpose of this example is to demonstrate the functionality of SWR for modeling a tightly coupled surface and groundwater system and to demonstrate the types of scenarios that can be simulated. The model uses a constant horizontal grid spacing of 500 m and simulates the period from January 1996 through December 1998. The area of interest is the area draining to and drained by Snapper Creek; active areas adjacent to Snapper Creek were included to minimize boundary effects in the area of interest. The relief in

17456584, 2015, 3, Downloaded from https://ngwa.onlinelibrary.wiley.com/doi/10.1111/gwat.12216 by U.S. Geological Survey Library, Wiley Online Library on [03/04/2024]. See the Terms and Conditions (https://onlinelibrary.wiley.com/terms-and-conditions) on Wiley Online Library for rules of use; OA articles are governed by the applicable Creative Commons License

the study area is low and the average topographic gradient in the active model domain is 3.36×10^{-4} m/m.

Daily Doppler radar-derived rainfall (NEXRAD) data, calibrated using rain-gauge precipitation measurements (Skinner et al. 2009), were applied to the model as potential groundwater recharge using the MODFLOW recharge (RCH) package. Daily Geostationary Operational Environmental Satellite (GOES) based reference evapotranspiration data (Mecikalski et al. 2011) were applied to the model as the maximum evapotranspiration rate using the MODFLOW evapotranspiration (EVT) package. Maximum evapotranspiration rates occur when the simulated water level in an active model cell is at or above land surface (the top of model layer 1). Evapotranspiration rates decrease linearly to 0 m/d when the depth to water is greater than or equal to 1 m below land surface. NEXRAD and GOES data are available on identical meteorologic data grids, having 2000 × 2000 m cells, and were mapped to the model grid using a Reimann sum of meteorologic data cell areas within each model grid cell. Average annual rainfall and potential evapotranspiration rates in the study area were 1.070 and 1.279 m/year, respectively.

The surface water system was represented using a total of 629 rectangular, diffusive-wave reaches, with constant Gauckler-Manning-Strickler roughness coefficients of 0.03 $s/m^{1/3}$ and variable bottom width data from Giddings et al. (2006), and 26 surface water control structures (Figure 5B). The location, geometry, pumping rate, and structure coefficients for the surface water control structures are provided in the Supporting Information. Surface water control structures along the western boundary of the model were used to supply water to recharge municipal wellfields and control saltwater intrusion; the western structures were simulated as specified flow structures using daily discharge data calculated by the South Florida Water Management District from breakpoint upstream and downstream stages, breakpoint gate opening data, and structure dimensions. All other simulated surface water control structures were operated using breakpoint gate opening data or operational control elevations for structures without breakpoint gate opening data (South Florida Water Management District 2002).

Reach conductance was dynamically calculated using aquifer properties and a channel bed leakance of 10/d. Daily observed downstream stage data from the southernmost coastal surface water control structure were applied to the downstream reach of all surface water features discharging to Biscayne Bay as a specified-stage boundary condition. Adaptive time steps ranging from 30 s to 1 d were used in the surface water domain.

The groundwater component of the model was derived from a model of eastern Miami-Dade County developed to determine the capture zones for two municipal wellfields (Brakefield et al. 2013). The Biscayne aquifer is represented as a single model layer with hydraulic conductivities based on data from Fish and Stewart (1991) and Renken et al. (2008). The model domain includes the five municipal wellfields, which had an average combined groundwater withdrawal rate of 7.536 m^3/s during the simulation period (Figure 5B). Lateral groundwater boundary conditions were specified along the eastern and western edges of the model domain, which represent natural hydraulic boundaries provided by Biscayne Bay and the Everglades, respectively (Figure 5B). Time series of groundwater heads from two observation wells representative of water levels in the northern (3BS1W1) and southern (G-3772) portions of the Everglades adjacent to the study area were used to define transient heads for the general head boundaries along the western external boundary of the active model domain. Daily observed downstream stage data from the southernmost coastal surface water control structure were also used to define the stage for general head boundaries representing water levels in Biscayne Bay. A conductance value of 2.5×10^6 m^2/d was assigned to all general head boundaries. No-flow boundaries were applied along the northern and southern edges of the model domain; the northern and southern edges of the model correspond to surface water basin boundaries, roughly coincide with groundwater basin boundaries, and are roughly parallel with groundwater-flow directions. Daily stress periods, with a single time step per stress period, were used in the groundwater domain.

The Snapper Creek model was not calibrated. However, Biscayne aquifer hydraulic properties used in the Snapper Creek model are from the model of Brakefield et al. (2013), which was calibrated using daily groundwater observations and estimated base flow. Additional details on Biscayne aquifer hydraulic properties and model calibration are available in Brakefield et al. (2013).

Simulated average annual net groundwater recharge, the difference between NEXRAD rainfall data applied in the RCH package and model-simulated evapotranspiration calculated by the EVT package, was 0.8826 m/year. The spatial distribution of average annual net groundwater recharge rates are provided in the Supporting Information.

Simulated upstream stages at the S-22 surface water control structure are approximately 0.6 m higher than downstream stages (Figure 6A). The S-22 surface water control structure represents the downstream freshwater discharge point for Snapper Creek. S-22 is closed more than half of the simulation period but when open can discharge more than 20 m^3/s following high-intensity rainfall events exceeding 0.05 m/d (Figure 6B). Simulated groundwater levels in the cell underlying S-22 are generally less than the upstream stage at S-22 except after high-intensity rainfall events when groundwater levels can equal or exceed the upstream stage (Figure 6A).

The Biscayne Bay boundary condition was increased by 0.25 m to quantify the response of the surface water and groundwater system to a 0.25-m sea-level increase. No other modifications were made to the Snapper Creek model. Simulated upstream stages and groundwater levels increase an average of 0.11 and 0.17 m, respectively, in response to a 0.25 m sea-level increase (Figure 7A). Increased sea level reduced average Snapper Creek discharge through S-22 by 0.27 m^3/s and by as much as 3.81 m^3/s (Figure 7B). The cumulative discharge reduction per

17456584, 2015, 3, Downloaded from https://ngwa.onlinelibrary.wiley.com/doi/10.1111/gwat.12216 by U.S. Geological Survey Library, Wiley Online Library on [03/04/2024]. See the Terms and Conditions (https://onlinelibrary.wiley.com/terms-and-conditions) on Wiley Online Library for rules of use; OA articles are governed by the applicable Creative Commons License

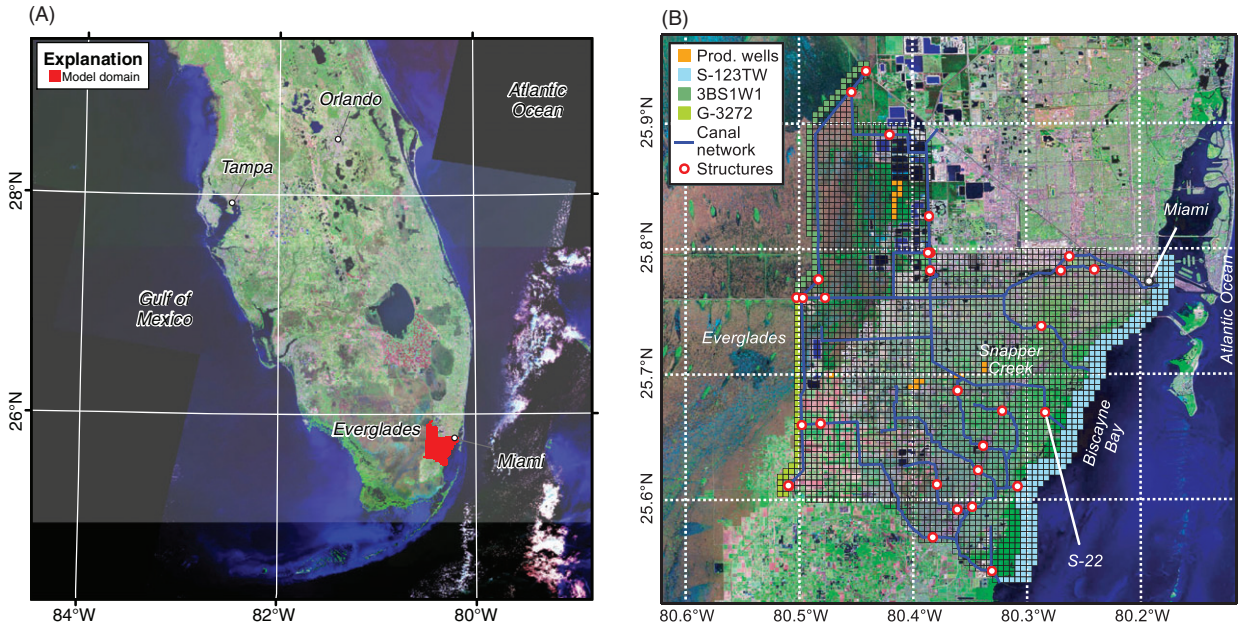

Figure 5. (A) Map showing the location of the Snapper Creek area of Miami-Dade County, Florida. (B) Map showing the Snapper Creek area of Miami-Dade County, the surface water canal network, the location of surface water control structures, and the groundwater model grid. The location of groundwater model cells with external general head boundary conditions (S-123TW, 3BS1W1, and G-3272) and production wells are also shown in (B).

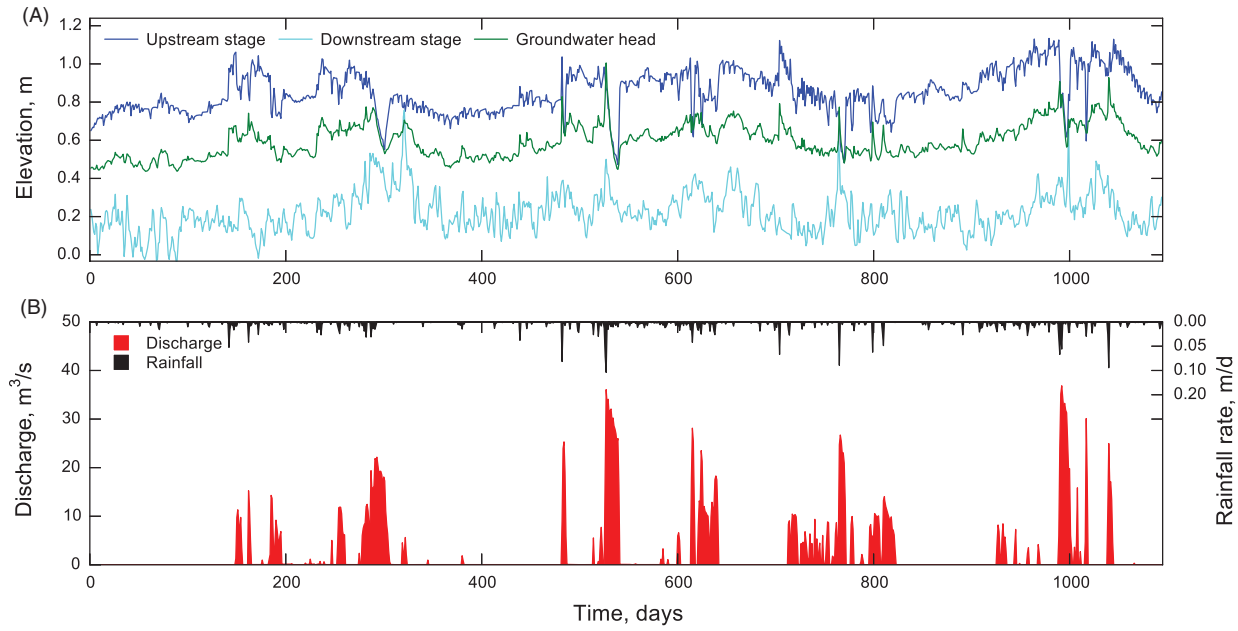

Figure 6. (A) Simulated stage upstream and downstream of surface water control structure S-22. Simulated groundwater level in the model cell underlying S-22 is also shown in (A). (B) Specified rainfall in the model domain and simulated discharge through S-22.

unit area (1.65×10^8 m^2) at the end of the simulation period was 0.1544 m, approximately 9% of average annual net groundwater recharge. Reduction in Snapper Creek discharge was a result of decreased hydraulic gradients across the model domain caused by increased sea level in Biscayne Bay (Figure 8). At the end of the simulation period, increased sea level caused a 0.11-m increase in the average groundwater level in active model cells. Decreased hydraulic gradients under increased sea-level conditions resulted in a 10 and 7% reduction in Biscayne aquifer seepage to the surface water system and surface water discharge to Biscayne Bay, respectively. Similarly, decreased surface water and groundwater gradients under increased sea-level conditions resulted in a 5, 10, and 17% reduction in groundwater inflow from the Everglades, surface water leakage to the Biscayne aquifer,

17456584, 2015, 3, Downloaded from https://ngwa.onlinelibrary.wiley.com/doi/10.1111/gwat.12216 by U.S. Geological Survey Library, Wiley Online Library on [03/04/2024]. See the Terms and Conditions (https://onlinelibrary.wiley.com/terms-and-conditions) on Wiley Online Library for rules of use; OA articles are governed by the applicable Creative Commons License

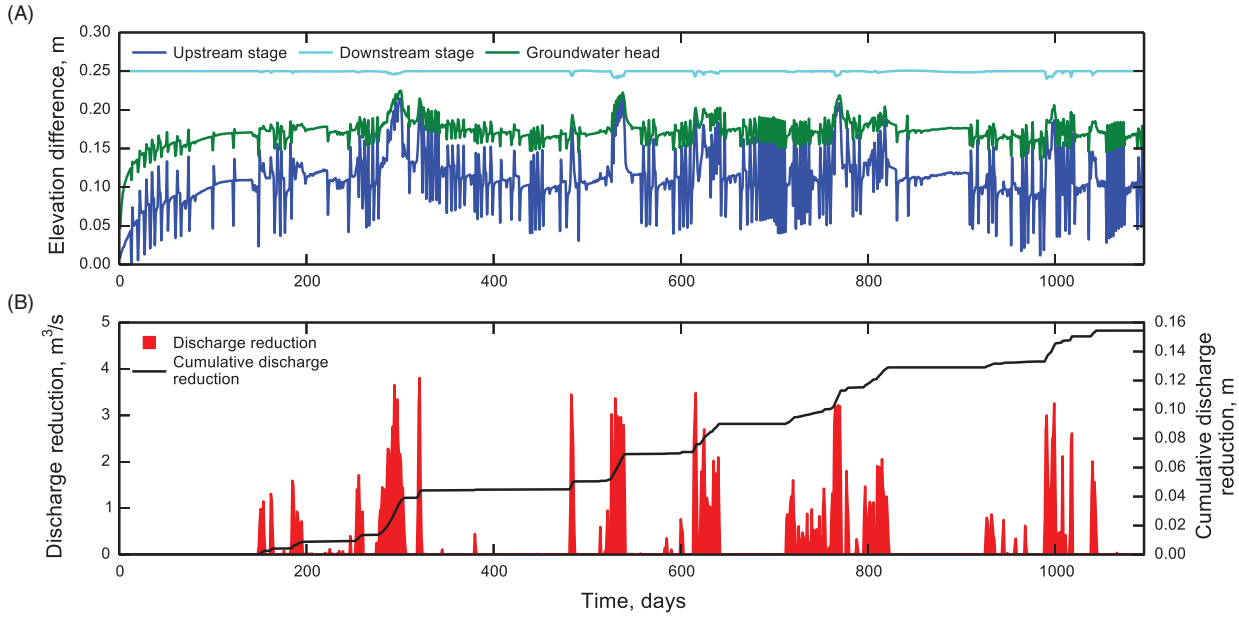

Figure 7. (A) Simulated difference in stage upstream and downstream of surface water control structure S-22 between the 0.25-m increase and base sea-level conditions. Simulated difference in groundwater level in the model cell underlying S-22 between the 0.25-m increase and base sea-level conditions is also shown in (A). (B) Simulated daily and cumulative reduction in discharge between the 0.25-m increase and base sea-level conditions.

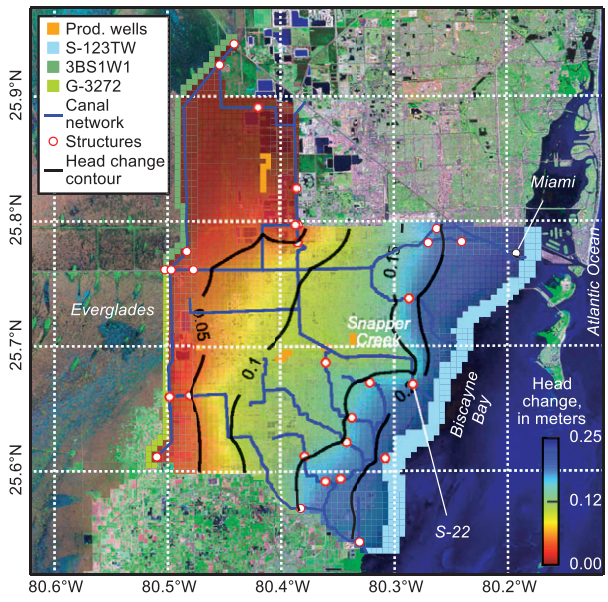

Figure 8. Map of simulated difference in groundwater levels between the 0.25-m increase and base sea-level conditions in the Snapper Creek area of Miami-Dade County. Head difference contours (0.05 m contour interval) are also shown.

and groundwater discharge to Biscayne Bay, respectively. Conversely, increased sea-level conditions resulted in a 5 and 1% increase in evapotranspiration and Biscayne aquifer storage, respectively.

Brakefield et al. 2013 evaluated the effects of a proposed seepage barrier between the Everglades and urban areas of Miami-Dade County and expansion of rock mining activities just east of the Everglades on wellfield capture zones. Surface water features were represented using the MODFLOW river (RIV) package (Harbaugh 2005), which uses specified stages (that can vary by stress period) to simulate surface water/groundwater interactions. Use of the SFR2 package was not an option because of the low topographic gradient and extensive use of surface water control structures in the study area. It is reasonable to expect that surface water stages would be affected by the scenarios evaluated by Brakefield et al. (2013). As a result, the accuracy of the scenario results of Brakefield et al. (2013) is uncertain because of the use of specified stages in the RIV package. Use of a combined SWR-MODFLOW simulation to evaluate these scenarios would likely reduce the uncertainty of the scenarios evaluated by Brakefield et al. (2013).

Summary

SWR is a numerical model that can simulate surface water routing using a diffusive-wave approximation of the Saint-Venant equations and/or a simplified level-pool approach. Backwater conditions caused by small surface water gradients or surface water control structures can be simulated in SWR. The nonlinear surface water flow equations implemented in SWR are solved using Newton methods and either direct or iterative solvers. SWR has been implicitly coupled to MODFLOW and the combination of these two codes can be used to simulate dynamic surface water/groundwater interactions in low-gradient surface water systems. The addition of SWR to MODFLOW supplements the capabilities of the existing SFR2 package, which can be simultaneously applied to surface water features where stream discharge is a function of channel bed slope.

17456584, 2015, 3, Downloaded from https://ngwa.onlinelibrary.wiley.com/doi/10.1111/gwat.12216 by U.S. Geological Survey Library, Wiley Online Library on [03/04/2024]. See the Terms and Conditions (https://onlinelibrary.wiley.com/terms-and-conditions) on Wiley Online Library for rules of use; OA articles are governed by the applicable Creative Commons License

SWR has been tested previously with a number of surface water flow problems but has been compared to three additional test problems in this study. We have evaluated SWR results for an axisymmetric overland flow problem, the tilted V-catchment overland flow problem, and the modified Pinder-Sauer surface water/groundwater interaction problem. SWR was compared to results from other numerical codes or in the case of the modified Pinder-Sauer problem an analytical solution. Comparisons for these three numerically challenging problems indicate that SWR is capable of providing accurate solutions. Differences between SWR and previous studies can be attributed to: (1) differences between the approach SWIFT2D uses to calculate surface water gradients (axisymmetric overland flow problem), (2) numerical methods (finite-volume vs. finite-element—V-catchment overland flow problem), and (3) initial conditions (Pinder-Sauer problem).

Results for an uncalibrated combined SWR-MODFLOW model for the Snapper Creek area of Miami-Dade County provides a field example that uses both SWR and MODFLOW to evaluate how surface water and groundwater systems might respond to future hydrologic conditions. The effect of a 0.25-m sea-level increase on surface water discharge and groundwater levels was evaluated. Increased sea level increased groundwater levels, increased evapotranspiration, decreased hydraulic gradients, decreased surface water discharge to Biscayne Bay, decreased groundwater discharge to Biscayne Bay, and decreased surface water/groundwater exchanges. It would be difficult to determine the effect of a 0.25-m sea-level increase on the surface water and groundwater systems without SWR because of the tight coupling of the two systems and extensive use of surface water control structures in the Snapper Creek area of Miami-Dade County.

Acknowledgments

The authors would like to acknowledge Alden M. Provost for his suggestions on approaches for accurately simulating axisymmetric surface water flow problems. Paul Juckem of the USGS provided a careful and thoughtful review of an earlier version of this article. The authors are also grateful to the editor and two anonymous reviewers for their valuable suggestions and comments.

Supporting Information

Additional Supporting Information may be found in the online version of this article:

Table S1. Surface water control structures in the Snapper Creek area of Miami-Dade County Florida.
Figure S1. Snapper Creek net groundwater recharge during the simulation period in millimeters per year.

References

Brakefield, L., J.D. Hughes, C.D. Langevin, and K. Chartier. 2013. Estimation of capture zones and drawdown at the Northwest and West Well Fields, Miami-Dade County, Florida, using an unconstrained Monte Carlo analysis: recent (2004) and proposed conditions. U.S. Geological Survey Open-File Report 2013–1086, 124 p. Reston, Virginia: USGS.

Chin, D.A. 1991. Leakage of clogged channels that partially penetrate surficial aquifers. *Journal of Hydraulic Engineering* 117, no. 4: 467–488. DOI:10.1061/(ASCE)0733-9429(1991)117:4(467).

Di Giammarco, P., E. Todini, and P. Lamberti. 1996. A conservative finite elements approach to overland flow: The control volume finite element formulation. *Journal of Hydrology* 175, no. 1–4: 267–291. DOI:10.1016/S0022-1694(96)80014-X.

Faunt, C.C. 2009. Groundwater availability of the Central Valley Aquifer, California. U.S. Geological Survey Professional Paper 1766, 227 p. Reston, Virginia: USGS.

Feng, K., and F.J. Molz. 1997. A 2-D, diffusion-based, wetland flow model. *Journal of Hydrology* 196: 230–250.

Fish, J.E., and M.T. Stewart. 1991. Hydrogeology of the surficial aquifer system, Dade County, Florida. U.S. Geological Survey Water-Resources Investigations Report 90-4108. Reston, Virginia: USGS.

Giddings, J.B., L.L. Kuebler, J.I. Restrepo, K.A. Rodberg, A.M. Montoya, and H.A. Radin. 2006. Draft report of Lower East Coast subregional (LECsR) MODFLOW model documentation. South Florida Water Management District, 294 p.

Harbaugh, A.W. 2005. MODFLOW-2005, the U.S. Geological Survey modular ground-water model – The ground-water flow process. U.S. Geological Survey Techniques and Methods 6-A16, variously paged. Reston, Virginia: USGS.

Höffmann, J., S.A. Leake, D.L. Galloway, and A.M. Wilson. 2003. MODFLOW-2000 ground-water model – User guide to the subsidence and aquifer-system compaction (SUB) package. U.S. Geological Survey Open-File Report 03-233, 44 p. Reston, Virginia: USGS.

Hughes, J.D., C.D. Langevin, K.L. Chartier, and J.T. White. 2012. Documentation of the surface-water routing (SWR1) process for modeling surface-water flow with the U.S. Geological Survey modular ground-water model (MODFLOW-2005). U.S. Geological Survey Techniques and Methods, Book 6, Chapter A40 (Version 1.0), 113 p. Reston, Virginia: USGS.

Hughes, J.D., J.D. Decker, and C.D. Langevin. 2011. Use of upscaled elevation and surface roughness data in two-dimensional surface water models. *Advances in Water Resources* 34, no. 9: 1151–1164. DOI:10.1016/j.advwatres.2011.02.004.

Lal, A.M.W. 2001. Modification of canal flow due to stream-aquifer interaction. *Journal of Hydraulic Engineering* 127, no. 7: 567–576. DOI:10.1061/(ASCE)0733-9429(2001)127:7(567).

Lal, A.M.W. 1998. Weighted implicit finite-volume model for overland flow. *Journal of Hydraulic Engineering* 124, no. 9: 941–950. DOI:10.1061/(ASCE)0733-9429(1998)124:9(941).

Leake, S.A., and D.L. Galloway. 2007. MODFLOW ground-water model – User guide to the subsidence and aquifer-system compaction package (SUB-WT) for water-table aquifers. U.S. Geological Survey, Techniques and Methods 6–A23, 42 p. Reston, Virginia: USGS.

Lee, T.M., L.A. Sacks, and J.D. Hughes. 2010. Effects of groundwater levels and headwater wetlands on streamflow in the Charlie Creek basin, Peace River watershed, west-central Florida. U.S. Geological Survey Scientific Investigations Report 2010–5189, 77 p. Reston, Virginia: USGS.

Mecikalski, J.R., D.M. Sumner, J.M. Jacobs, C.S. Pathak, S.J. Paech, and E.M. Douglas. 2011. Use of visible geostationary operational meteorological satellite imagery

17456584, 2015, 3, Downloaded from https://ngwa.onlinelibrary.wiley.com/doi/10.1111/gwat.12216 by U.S. Geological Survey Library, Wiley Online Library on [03/04/2024]. See the Terms and Conditions (https://onlinelibrary.wiley.com/terms-and-conditions) on Wiley Online Library for rules of use; OA articles are governed by the applicable Creative Commons License

in mapping reference and potential evapotranspiration over Florida. In *Evapotranspiration*, ed. L. Labedzki, 229–254. Rijeka, Croatia: InTech. DOI: 10.5772/14478.

Nemeth, M.S., and H.M. Solo-Gabriele. 2003. Evaluation of the use of reach transmissivity to quantify exchange between groundwater and surface water. *Journal of Hydrology* 274, no. 1–4: 145–159. DOI:10.1016/S0022-1694(02)00419-5.

Niswonger, R.G., S. Panday, and M. Ibaraki. 2011. MODFLOW-NWT, A Newton formulation for MODFLOW-2005. U.S. Geological Survey Techniques and Methods, Book 6, Chapter A37, 44 p. Reston, Virginia: USGS.

Niswonger, R.G., D.E. Prudic, and R.S. Regan. 2006. Documentation of the unsaturated-zone flow (UZF1) package for modeling unsaturated flow between the land surface and the water table with MODFLOW-2005. U.S. Geological Survey Techniques and Methods, Book 6, Chapter A19, 62 p. Reston, Virginia: USGS.

Niswonger, R.G., and D.E. Prudic. 2005. Documentation of the streamflow-routing (SFR2) package to include unsaturated flow beneath streams – A modification to SFR1. U.S. Geological Survey Techniques and Methods, Book 6, Chapter A13, 47 p. Reston, Virginia: USGS.

Panday, S., and P.S. Huyakorn. 2004. A fully coupled physically-based spatially-distributed model for evaluating surface/subsurface flow. *Advances in Water Resources* 27, no. 4: 361–382. DOI:10.1016/j.advwatres.2004.02.016.

Pinder, G.F., and S.P. Sauer. 1971. Numerical simulation of flood wave modification due to bank storage effects. *Water Resources Research* 7, no. 1: 63–70. DOI:10.1029/WR007i001p00063.

Renken, R.A., K.J. Cunningham, A.M. Shapiro, R.W. Harvey, M.R. Zygnerski, D.W. Metge, and M.A. Wacker. 2008. Pathogen and chemical transport in the karst limestone of the Biscayne aquifer: 1. Revised conceptualization of groundwater flow. *Water Resources Research* 44: W08429. DOI:10.1029/2007WR006058.

Schaffranek, R.W. 2004. Simulation of surface-water integrated flow and transport in two dimensions: SWIFT2D user's manual. U.S. Geological Survey Techniques and Methods, 6 B-1, 115 p. Reston, Virginia: USGS.

Schmid, W., R.T. Hanson, T. Maddock III, and S.A. Leake. 2006. User guide for the farm process (FMP1) for the U.S. Geological Survey's modular three-dimensional finite-difference ground-water flow model, MODFLOW-2000. Geological Survey Techniques and Methods 6-A17, 127 p. Reston, Virginia: USGS.

Skinner, C., F. Bloetscher, and C.S. Pathak. 2009. Comparison of NEXRAD and rain gauge precipitation measurements in South Florida. *Journal of Hydrologic Engineering* 14, no. 3: 248–260. DOI:10.1061/(ASCE)1084-0699(2009)14:3(248).

South Florida Water Management District. 2002. *Structure Books*. West Palm Beach, Florida: South Florida Water Management District.

Swain, E.D., and E.J. Wexler. 1996. A coupled surface-water and ground-water flow model (MODBRANCH) for simulation of stream-aquifer interaction. U.S. Geological Survey Techniques of Water-Resources Investigations Report, Book 6, Chapter A6, 125 p. Reston, Virginia: USGS.

Zoppou, C. 1999. Reverse routing of flood hydrographs using level pool routing. *Journal of Hydrologic Engineering* 4, no. 2: 184–188.

The history of hydrogeology available at your fingertips.

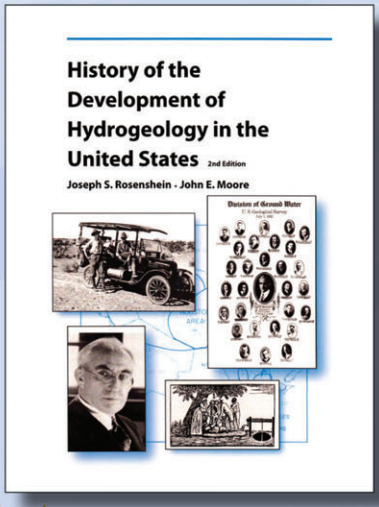

No hydrogeology library would be complete without the recently published reference volume *History of the Development of Hydrogeology in the United States* written by retired USGS hydrogeologists Joseph S. Rosenshein and John E. Moore.

Emphasizing the contributions of the scientific community from 1776 to 2010, this NGWA® Press book not only provides a comprehensive perspective on the development of this field of study, it also discusses hydrologic education, the influence of professional societies, groundwater contamination, chemical hydrogeology, and other aspects of hydrogeology.

Order your copy today!

History of the Development of Hydrogeology in the United States
Catalog #T1097
NGWA member price $40.00
Nonmember price $50.00

national ground water association

www.NGWA.org/Bookstore • 800 551.7379 • 614 898.7791

17456584, 2015, 3, Downloaded from https://ngwa.onlinelibrary.wiley.com/doi/10.1111/gwat.12216 by U.S. Geological Survey Library, Wiley Online Library on [03/04/2024]. See the Terms and Conditions (https://onlinelibrary.wiley.com/terms-and-conditions) on Wiley Online Library for rules of use; OA articles are governed by the applicable Creative Commons License